tvst

Article

Developing a Screening Tool for Areas of Abnormal Central Vision Using Visual Stimuli With Natural Scene Statistics

Rekha Srinivasan[1], Andrew Turpin[2], and Allison M. McKendrick[1]

[1] Department of Optometry and Vision Sciences, The University of Melbourne, Parkville, Victoria, Australia
[2] School of Computing and Information Systems, The University of Melbourne, Parkville, Victoria, Australia

Correspondence: Allison M. McKendrick, Department of Optometry & Vision Sciences, The University of Melbourne, Parkville, Vic 3010, Australia.
e-mail: allisonm@unimelb.edu.au

Received: September 8, 2021
Accepted: January 24, 2022
Published: February 23, 2022

Keywords: screening; visual field; fixation; visual search; natural scenes

Citation: Srinivasan R, Turpin A, McKendrick AM. Developing a screening tool for areas of abnormal central vision using visual stimuli with natural scene statistics. Transl Vis Sci Technol. 2022;11(2):34, https://doi.org/10.1167/tvst.11.2.34

Purpose: Previous studies show that some visual field (VF) defects are detectable from visual search behavior; for example, when watching video. Here, we developed and tested a VF testing approach that measures the number of fixations to find targets on a background with spatial frequency content similar to natural scenes.

Methods: Twenty-one older controls and 20 people with glaucoma participated. Participants searched for a Gabor (6 c/°) that appeared in one of 25 possible locations within a 15° (visual angle) 1/f noise background (RMS contrast: 0.20). Procedure performance was assessed by calculating sensitivity and specificity for different combinations of control performance limits (p = 95%, 98%, 99%), number of target locations with fixations outside control performance limits ($k = 0$ to 25) and number of repeated target presentations ($n = 1$ to 20).

Results: Controls made a median of two to three fixations (twenty-fifth to seventy-fifth percentile: two to four) to locate the target depending on location. A VF was flagged "abnormal" when the number of fixations was greater than the $p = 99\%$ for $k = 3$ or more locations with $n = 2$ repeated presentations, giving 85% sensitivity and 95.2% specificity. The median test time for controls was 85.71 (twenty-fifth to seventy-fifth percentile: 66.49–113.53) seconds.

Conclusion: Our prototype test demonstrated effective and efficient screening of abnormal areas in central vision.

Translational Relevance: Visual search behavior can be used to detect central vision loss and may produce results that relate well to performance in natural visual environments.

Introduction

Assessment of visual field loss is a common clinical requirement. Although visual field loss can present in many forms, damage to the central visual field has been found to have a specific, direct impact on daily living activities.[1–4] Typically, routine visual field assessments are performed using static automated perimetry that measures contrast detection performance for luminance increment targets presented on uniform luminance backgrounds.[5,6] Static automated perimetry has several requirements of people that are not representative of typical visual behavior. For example, people are required to maintain steady central fixation throughout testing, rather than making more natural eye movements. Consequently, patients often complain of Troxler fading,[7] discomfort, and fatigue during or after the assessment.[8] Another key difference between clinical visual field tests and natural visual environments is that natural scenes typically have objects of interest embedded in more complex backgrounds. There is evidence that standard measures of vision across the visual field may not predict visual performance in more natural environments.[9–11] Current clinical visual field tests also have limitations relating to the need for specialized, expensive hardware, and a need for training on the task, possibly necessitated by the relatively unnatural visual task requirements.

To address some of the limitations of current visual field testing procedures, several recent studies have

developed alternative approaches to measure or screen for visual field loss by incorporating visual search behavior.[12–16] For example, to assess patients' visual search performance in everyday life, the pattern of natural eye movements such as number of saccades, number of fixations, saccadic amplitude, and saccadic latency was evaluated in control participants and people with visual field loss in scenarios such as watching TV/movies,[17] reading,[18–21] driving,[22–25] and viewing objects in everyday scenes.[26–29] The general conclusion of this body of work is that people with glaucoma show abnormal patterns of visual search behavior in visually complex environments, depending on the severity and the type of visual field loss. However, because widely varying visual content is presented in stimuli such as movies or photographs (for example, widely varying basic visual attributes such as spatial, color and motion cues, in addition to higher level attributes such as differences in object scene gist), it is highly complex to make specific predictions of performance for any individual visual scene.

In this study, we develop and test a new method for screening for central visual field loss that requires people to visually search for targets on a background that is designed to represent natural image statistics but that does not contain specific objects within the image content. We chose this particular approach because of the availability of an established theoretical framework linking target detectability within the image to the predicted number of fixations.[30] Here, we present a screening protocol that is based on counting the number of fixations to find targets on a background with spatial frequency content similar to natural scenes (referred to as 1/f noise).[31] We also evaluated whether the developed prototype test was able to detect central visual field loss in a group of glaucoma participants. In this study, we recruited people with glaucoma, an age-related neurodegenerative disease that is known to cause visual field loss. However, the current study results are not specific for glaucomatous central visual field loss and can be applied to other visual conditions that affect central vision.

Methods

Participants

Twenty-one control participants (age range, 61–79 years) and 20 people with glaucoma (age range, 59–84 years) were recruited. There was no significant difference (independent t-test, $t_{39} = 1.81$, $P = 0.078$) in the mean age between the groups (control, mean [± standard deviation {SD}] age = 69 ± 5.58 years; glaucoma, mean [± SD] age = 72.5 ± 6.45 years). All participants underwent a complete ocular examination to ensure study eligibility, including visual acuity measurement (Early Treatment Diabetic Retinopathy Study chart), slit lamp biomicroscopy, and ophthalmoscopy. In addition to the complete ocular examination, all participants underwent optic nerve head and macula assessment using the Heidelberg Spectralis with the Glaucoma Module (Heidelberg Engineering GmBH, Heidelberg, Germany) and central visual field assessment using a Humphrey Field Analyzer (HFA 10-2 SITA Standard; Carl Zeiss Meditec, Dublin, CA, USA). All 41 participants were required to meet the following inclusion criteria: best-corrected visual acuity better than or equal to 6/9.6 Snellen acuity (0.20 log MAR equivalent), distance refractive error within ± 5.00 D sphere or less than −2.00 D cylinder, and normal ocular health. Participants with glaucoma were required to have a clinical diagnosis of glaucoma with established visual field defects using the 24-2 test pattern assessed using SITA Standard (HFA). The optical coherence tomography (OCT) data were not used for inclusion purposes for the glaucoma group; however, control participants were required to have macular scans that were deemed normal by visual inspection using the Spectralis OCT (Heidelberg Engineering, GmBH, Heidelberg, Germany). Participants taking any medication known to affect contrast sensitivity or eye movements were excluded from the study. The study was approved by the Human Research Ethics Committee of the University of Melbourne (HREC Ethics ID 1750215.3). Written informed consent was obtained from the participants before the experiment, and all study protocols were in accordance with the tenets of the Declaration of Helsinki.

Apparatus

The experimental software was coded in Psychopy V1.85.2[32] and the stimuli were presented on a 32-inch gamma-corrected Display++ monitor (Cambridge Research Systems Ltd., Rochester, UK) with a refresh rate of 120 Hz, resolution of 1920 × 1080 pixels and a mean luminance of 50 cd/m^2. The fixations made to locate the targets were simultaneously monitored using a Gazepoint GP3 eye tracker (GP3, Software version V4.0.13; Gazepoint, Vancouver, Canada) with a sample rate of 60 Hz. Participants were seated at 80 cm from the monitor using a chin rest to maintain steady chin and head position. Individual refractive correction for 80 cm in a trial frame was provided while performing the test.

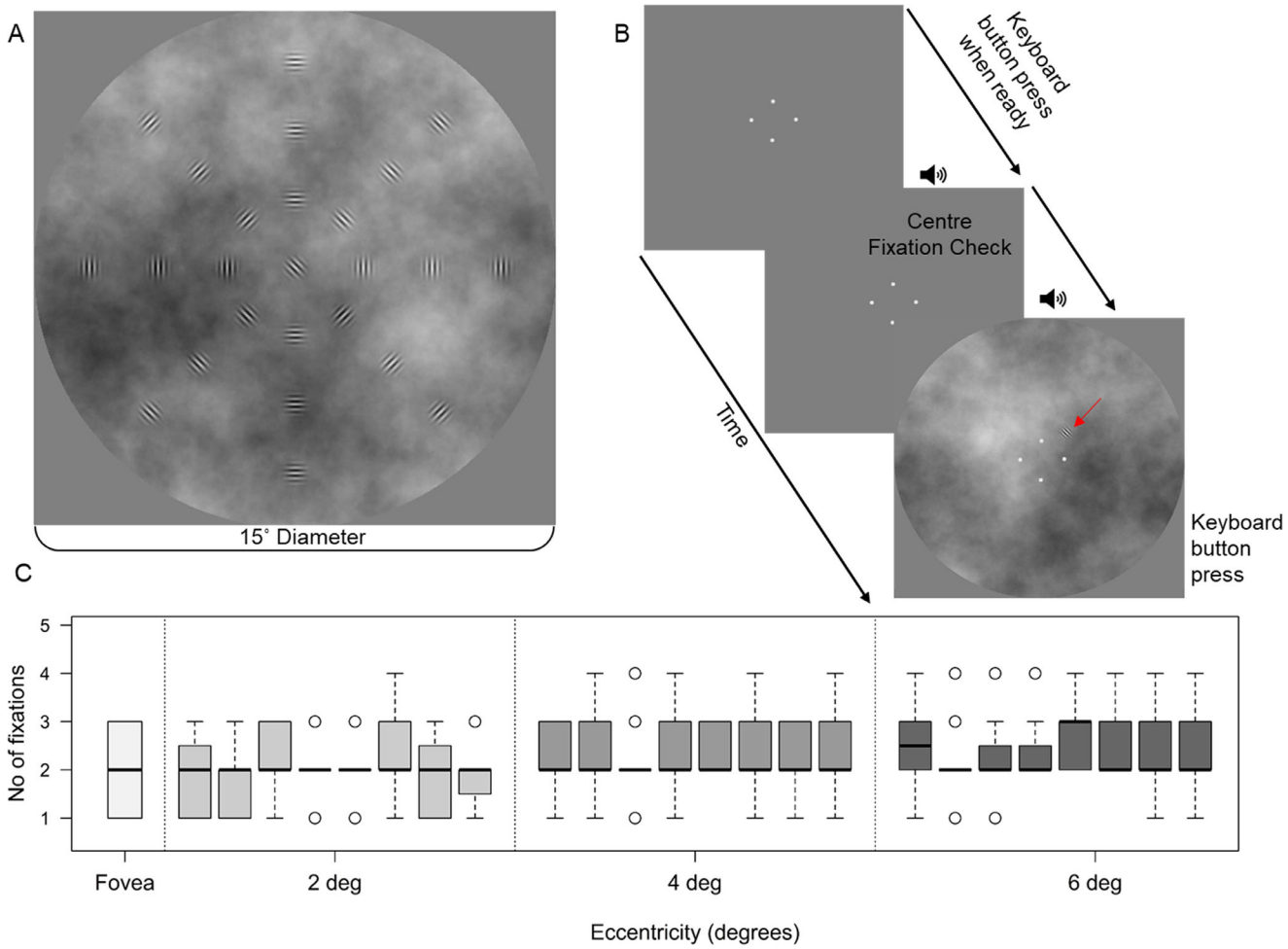

Figure 1. (**A**) Schematic illustration of the 1/f noise background and the locations at which the stimulus was presented.The stimulus was presented in one of the 25 locations for each presentation in the search task. (**B**) An example of stimulus presentation sequence for the visual search task determining the number of fixations to locate a stimulus on 1/f noise. (**C**) A result for one control participant (with normal visual field and visual acuity) with each box containing the number of fixations required to find the target at a location. The *box-whisker plot* represents data for 20 repeated presentations per location, with the *box* showing the twenty-fifth to seventy-fifth percentile, the *bold line* the median, *whiskers* the range up to 1.5 times the box length, and the *circles* extreme values.

Stimuli

The stimuli for the experiment were similar to those used by Najemnik and Geisler.[30] The 1/f noise background was designed to simulate the complex spatial frequency and orientation information of a natural scene. Natural scenes contain objects of varied orientation and spatial frequency content (biased toward low spatial frequencies) and are typically biased toward lower contrasts.[31,33,34] The power spectrum (2D representation of spatial frequency) of natural scenes is approximately proportional to the inverse of the frequency of the spectrum, and the relative log amplitude falls off roughly by a factor of 1/f.[31] Random filtered Gaussian noise images were initially created and then adjusted to the factor of $1/f^{\alpha}$ by setting the α value to 1.7 and an image size of 576 × 576 pixels (Fig. 1A). A total of 1000 noise images were created where root mean square (RMS) contrast was defined using two times the standard deviation of the normalized pixel luminance across the whole image and scaled to 0.20. Individual images were chosen at random from this bank of 1000 images, to be the background for the target in the screening test (described in detail in the next sections). At the viewing distance of 80 cm, the background images subtended 15 degrees of the visual field and the remainder of the screen was filled with gray (mean luminance of 50 cd/m^2) as shown in Figure 1A. The 1/f noise backgrounds used in this study were isotropic, and the visual search target was a six cycles

per degree Gabor patch (sine wave grating masked by a Gaussian distribution of SD 0.17°) oriented orthogonal to the visual field meridian as shown in Figure 1A.

Overview of Experimental Requirements

Each participant underwent two distinct tasks: (a) a repeated visual search task; (b) a contrast detection task. The order of the two tasks was randomized. Participants attended either one or two test sessions, each of approximately two hours duration, including training sessions and breaks. Two sessions were scheduled for several of the glaucoma participants for the following reasons: inability to complete all of the measurements in one session because of fatigue or greater than average practice required to familiarize with the task; strong participant preference to split into two testing sessions for logistical reasons. Each trial started with a calibration check where all participants performed a nine-point calibration followed by real-time validation of the gaze data. Calibration was considered to be acceptable when the nine calibration points were classified as valid according to the Gazepoint control software and the participant's gaze was within a calibration error of ±1° of visual angle. Calibration was repeated if these calibration criteria were not satisfied. Participants who did not meet the calibration criteria even after multiple attempts were not included in the study

Visual Search Protocol

All participants performed the visual search protocol (Fig. 1B) that measured the number of fixations to locate the Gabor patch on 1/f noise background. For each stimulus presentation, the participant was asked to look at the fixation target (small diamond, 1° radius white) at the center of the computer screen before the start of the experiment. The participants were instructed to start the task by a button press when looking at the central fixation. If the central fixation was within 1° tolerance of the fixation target, the stimulus presentation began with an auditory tone. If the central fixation was outside 1° tolerance, the participants were reinstructed to look at the center fixation target, and the stimulus presentation began after they had passed the fixation check. The fixation check at the beginning of each stimulus presentation was performed to ensure that all participants commenced the visual search from the center of the fixation target. After the central fixation check, participants were required to search for the Gabor patch embedded in the background 1/f noise (RMS noise 0.20). Once the participants located the target, they were asked to look at the target and simultaneously press the button to indicate their final fixation on the target. If the participant could not find the target despite searching, they were asked to press another button to indicate a "non-seen" target presentation.

Testing was performed monocularly where the dominant eye was chosen for the control group, and the worse eye as per the mean deviation of the 24-2 visual fields was chosen for the glaucoma group. The non-testing eye was patched through an Infrared-pass through filter to block the stimulus and also allow reliable gaze tracking. Throughout this document, we refer to a single stimulus presentation of the visual search protocol for each location as a presentation, a group of presentations involving 25 test locations (as shown in Fig. 1A) tested only once each as a trial, and a group of trials as an experimental run. The 1/f noise background was chosen at random from the 1000 created images (mentioned in an earlier section), with a new selection made for each presentation. A total of 20 trials were tested in the control group, and 10 to 15 trials were tested in the glaucoma group. The visual search task was repeated up to 20 times to collect data to pool to establish control performance limits and to determine the trade-off between test time and performance of different numbers of replicates, which was used as an input to the later specificity and sensitivity analysis. Note: it is not intended that any future application of the screening procedure would have so many replicates. For each presentation, the eye tracker provided the gaze points and the timestamp for each fixation. Gazepoint eye tracker uses a propriety algorithm based on displacement (correspondence from the manufacturer) to detect fixation. A position variance technique[35] is used where the sequence of gaze data spatially located within an area of interest over a specific time period is determined to belong to the current fixation. Any subsequent data outside this area is the beginning of a new fixation. The number of fixations for each presentation was estimated using the number of timestamps (detected as fixation by the eye tracker). The initial fixation from the center of the fixation marker was verified and included in the fixation count.

Contrast Detection Protocol

The contrast for the visual search stimulus was fixed at each location based on previously determined estimates of the stimulus contrast leading to 95% probability of seeing (methods described in Srinivasan et al.[36]) collected from a different dataset in older controls (N = 28). The contrast of the stimulus at each location was constant throughout the testing.

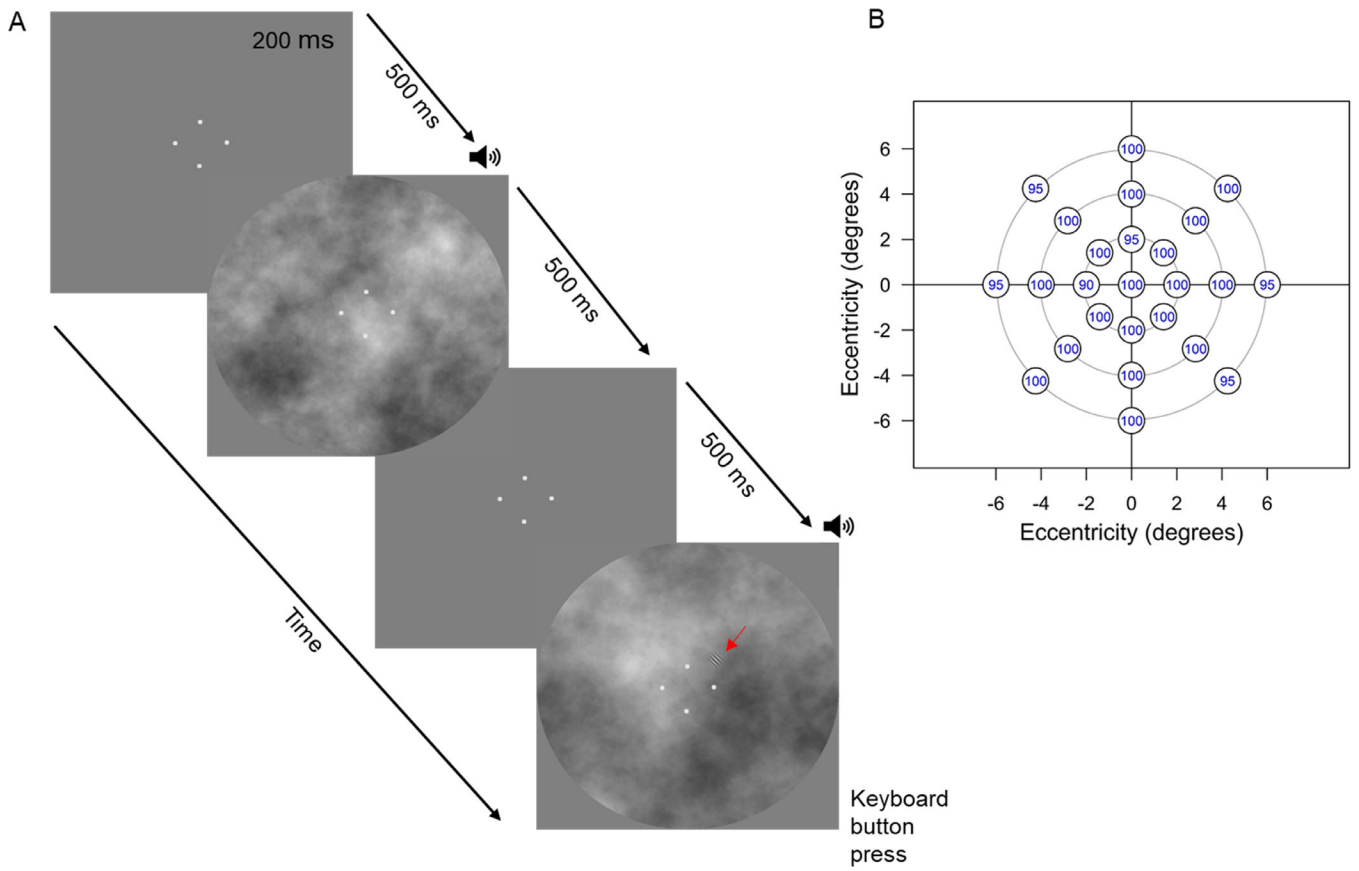

Figure 2. (**A**) A schematic of the stimulus and trial sequence for the two-interval forced-choice detection task. In this task, the interval of the noise image in which the participants saw the Gabor stimulus was recorded by a keyboard button press (for example, the second noise image). A gray background has been used in first and third image in the flowchart to represent mean luminance that was shown between the stimulus presentations. (**B**) Proportion of correct expressed as a percentage for the same control participant whose number of fixations are shown in Figure 1C.

In this experiment we measured the actual proportion of correct responses of these same targets for all participants in this study. The rationale was in part to confirm that the probability of correct for these stimuli was indeed suprathreshold for our new group of control participants and to allow analysis of the relation between the probability of correct and performance on the visual search task. That is, the data were used to confirm the validity of the approach; they were not designed to be part of the recommendations for the screening protocol.

Participants performed the detection protocol as a two-interval forced-choice procedure with a method of constant stimuli to estimate the proportion of correct responses for detecting the target at each location on the noise background (RMS contrast = 0.20). For each presentation, the participant was instructed to look at the fixation target (small diamond, 1° radius white) at the center of the computer screen. The target and the stimulus contrast were the same as the visual search task as shown in Figure 1A. At each presentation of the method of constant stimuli, the stimulus was presented at one of the 25 locations as shown in Figure 1A. After the presentation of the fixation target, a 1/f noise background appeared for 250 ms, which was followed by an interstimulus interval of 500 ms and then another 250 ms interval 1/f noise background (Fig. 2A). Each interval was distinguished by an auditory tone. The participants were asked to report the interval of the noise image in which they saw the Gabor stimulus by a keyboard button press (for example, the second noise image in Fig. 2A). A total of 20 trials were tested for the control group, and 10 to 15 trials were tested for the glaucoma group within the testing time frame. In the control group, to achieve 20 trials, four experimental runs were required where each run consisted of five trials (125 presentations) that took approximately five to six minutes per run. In the glaucoma group, two or three experimental runs were performed. Less data were collected on the glaucoma participants because

the visual screening task described above required a longer test duration in many of these people and the total session duration was limited for logistical and fatigue reasons. Rest breaks were offered between runs.

Data Analysis

Statistical analyses were conducted using R Version 3.4.4.[37] The proportion of correct, and the number of fixations were not normally distributed (Shapiro-Wilk test, $P < 0.001$) for both control and glaucoma groups. Therefore, for nonparametric measures, summary statistics are presented as the median with a measure of spread in brackets referring to the twenty-fifth and seventy-fifth percentile, respectively. The distribution of the number of fixations at all locations was positively skewed in the control group; therefore Gamma distributions were fit to the number of fixations at each location using *dgamma* function in R where the shape and rate parameters were adjusted by minimizing the sum of squared differences. From the fitted Gamma distributions, the 95%, 98%, and 99% control performance limits were derived using the *qgamma* function in R, and the values were rounded to the nearest whole number. For the purpose of making recommendations regarding future implementation as a screening procedure, we determined a criterion for the entire central visual field to be considered abnormal. Three parameters were explored to determine the criteria of abnormal: k represents the number of locations in which the number of fixations was outside the control performance limits at level p of either 95%, 98%, or 99%; and n is the number of trials required for the testing. Receiver operating characteristic curves were plotted to determine the specificity, sensitivity, and the area under the curve (AUC) for the screening approach for varied k values across each n and p value, with higher specificity, higher sensitivity, and a greater AUC being considered as the better performance.

Results

Figure 3A shows the median and interquartile range for the number of fixations made to locate the target across 25 locations determined by the visual search task for the control group. A median of two or three fixations was observed depending on location; this includes the initial fixation on the central fixation marker at the beginning of the presentation. The time taken (median) by the control participants to perform a single presentation for each location as per the stimulus sequence shown in Figure 1B was 1.68 (1.30–2.23) seconds, and the total time taken (median) by the participants in the control group to perform a trial containing 25 locations including the interstimulus interval of the visual search task was 42.86 (33.25–56.77) seconds. Figure 3B shows the median and

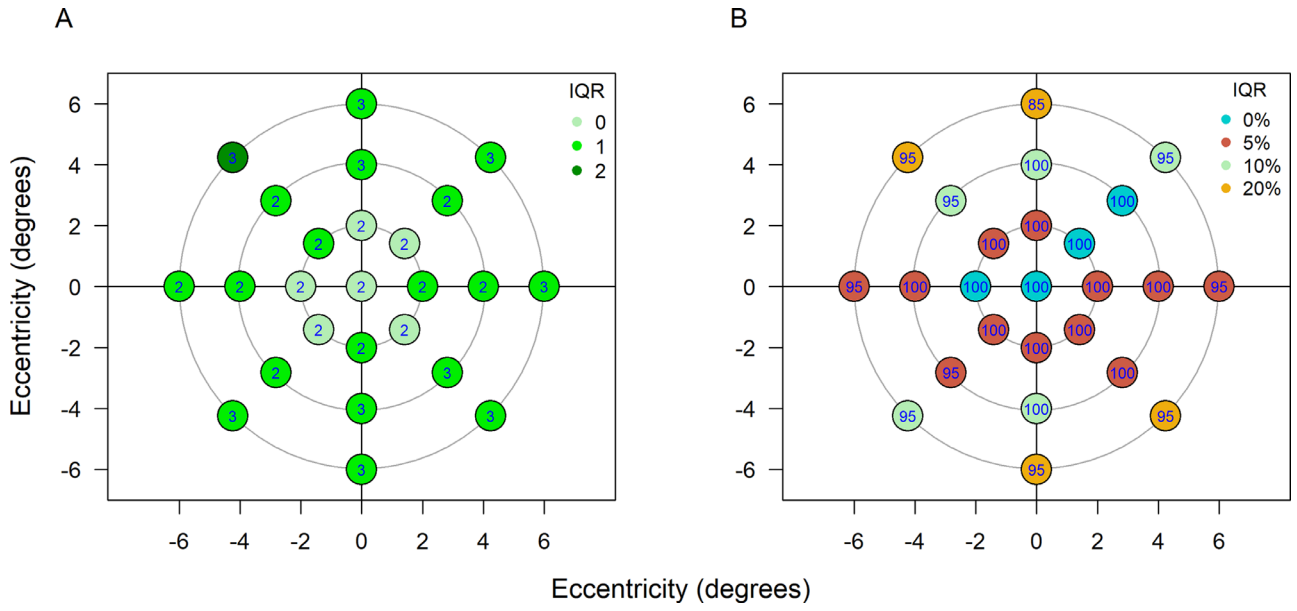

Figure 3. (**A**) Median and interquartile range across 21 control subjects for the number of fixations made to locate the target on the 1/f noise background at 25 locations at which the stimulus was presented. (**B**) Median and interquartile range across 21 control subjects for the proportion of correct on the 1/f noise background at 25 locations at which the stimulus was presented. The number inside the *small circles* represents the median value, and each *circle* is color coded based on their interquartile range (Quartile 3–Quartile 1).

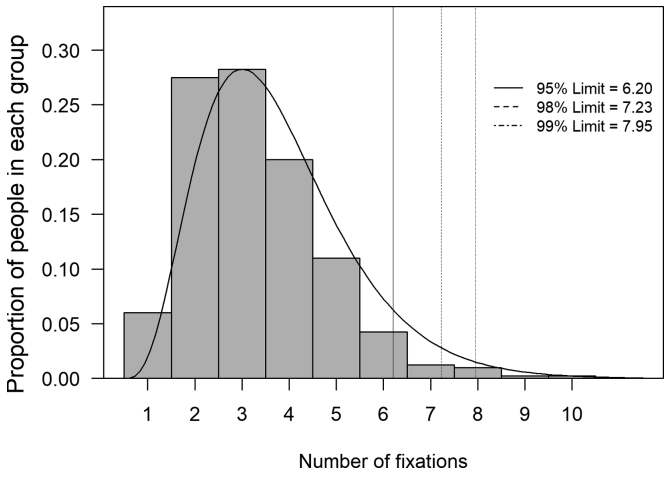

Figure 4. A histogram of the number of fixations required to find the target for an example target location (x,y coordinates = 0°, 6°). The solid curve is a fitted Gamma probability density function. The *solid vertical line* represents the 95% limit, *dashed vertical line* represents the 98% limit, and *dot-dashed vertical* represents the 99% limit for the number of fixations at that particular location.

interquartile range for the proportion of correct across 25 locations determined by the detection task in the control group expressed as a percentage. The median proportion of correct across 25 locations ranged from 85% to 100%. Figure 3B confirms that the stimuli chosen for the visual search task were super threshold in our control group and verifies the approach of setting the screening threshold from our previously collected data.[36]

Figure 3B confirms that the target was easily detectable by the control participants. For the visual search task, the number of fixations from all the trials in the control group was used to estimate the control performance limits (Fig. 3A). Figure 4 shows an example of how the control performance limits were derived for each location through fitting a Gamma distribution. For instance, in Figure 4, the 95% upper bound limit has a fixation number of 6; hence, individuals with a fixation number higher than 6 will be considered as outside the 95% control performance limits for that location. For each of the glaucoma participants, any fixation number higher than the control performance limits was considered abnormal for that location. The 95%, 98%, and 99% control performance limits of fixations for each location are provided in Supplementary Table S1.

After determining the control performance limits for each location, the data from glaucoma participants were used to assess the diagnostic ability of the screening test to identify areas of abnormal central vision. Figure 5 shows an example of the proportion of correct and the median number of fixations

Table 1. Sensitivities, pAUC, and the Criteria (*k*) for the Number of Locations to Be Flagged as Abnormal for Each *n* and *p* Value

Number of trials (*n*)	p = 95% Control Performance Limits			p = 98% Control Performance Limits			p = 99% Control Performance Limits		
	Criterion Location (*k*)	Sensitivity (95% CI) (%)	pAUC (95% CI)	Criterion Location (*k*)	Sensitivity (95% CI) (%)	pAUC (95% CI)	Criterion Location (*k*)	Sensitivity (95% CI) (%)	pAUC (95% CI)
$n = 1$	8	70 (50–90)	0.84 (0.69–0.97)	5	75 (55–90)	0.86 (0.73–0.97)	5	70 (50–90)	0.86 (0.73–0.97)
$n = 2$	10	70 (50–90)	0.84 (0.71–0.96)	4	85 (70–100)	0.87 (0.73–0.97)	3	85 (70–100)	0.88 (0.75–0.98)
$n = 3$	6	70 (50–90)	0.81 (0.65–0.96)	3	70 (50–90)	0.83 (0.71–0.94)	2	75 (55–90)	0.84 (0.73–0.95)
$n = 4$	9	65 (45–85)	0.80 (0.60–0.95)	3	80 (60–95)	0.85 (0.72–0.97)	2	75 (55–95)	0.84 (0.71–0.95)
$n = 5$	7	65 (45–85)	0.85 (0.72–0.97)	3	70 (50–90)	0.84 (0.72–0.95)	2	70 (50–90)	0.81 (0.70–0.93)
$n = 6$	9	65 (45–80)	0.84 (0.70–0.97)	4	65 (45–85)	0.84 (0.72–0.96)	3	65 (45–85)	0.81 (0.69–0.93)
$n = 7$	3	75 (55–90)	0.86 (0.72–0.97)	2	75 (55–90)	0.84 (0.71–0.95)	1	70 (50–90)	0.82 (0.70–0.93)
$n = 8$	3	80 (60–95)	0.86 (0.72–0.97)	2	75 (55–90)	0.85 (0.71–0.95)	1	75 (55–90)	0.83 (0.70–0.95)
$n = 9$	4	70 (50–90)	0.85 (0.71–0.96)	2	70 (50–90)	0.83 (0.71–0.93)	1	70 (45–85)	0.83 (0.71–0.93)
$n = 10$	3	75 (55–90)	0.85 (0.74–0.96)	3	70 (50–90)	0.82 (0.70–0.93)	1	70 (50–90)	0.83 (0.71–0.93)

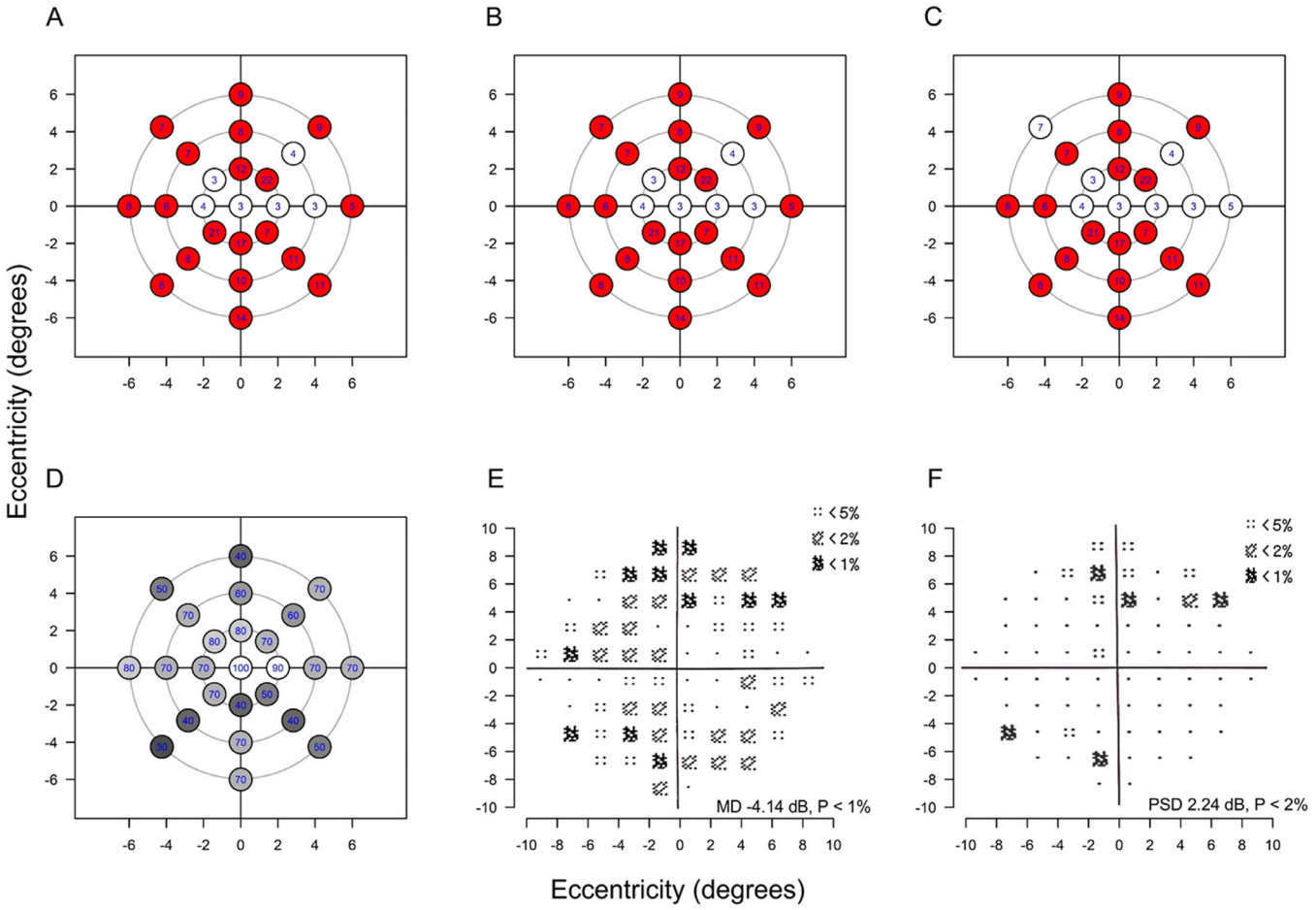

Figure 5. (**A–C**) An example of the visual search task output showing an average performance from a glaucoma participant where the small circles represent the median number of fixations made to locate the target on the 1/f noise background across 25 locations. *Red circles* represent the locations with the median number of fixations outside $p = 95\%$ (**A**), $p = 98\%$ (**B**), and $p = 99\%$ (**C**); *white circles* in A–C represent the locations with the median number of fixations within $p = 95\%$ (**A**), $p = 98\%$ (**B**), and $p = 99\%$ (**C**). (**D**) Same participant's proportion of correct on the 1/f noise background across 25 locations. The numbers inside the *small circles* represent the median proportion of correct. *White circles* represent the proportion of correct between 90% to 100%, *light gray circles* represent proportion of correct between 60% to 80%, and *darker gray circles* represent proportion of correct lower than 50%. (**E**) The total deviation plot and (**F**) the pattern deviation plot from the HFA 10-2 SITA standard result obtained from the same participant. MD, mean deviation; PSD, pattern standard deviation; dB, decibels.

over 20 trials from a glaucoma participant and illustrates locations where the fixation number falls outside normal limits. For this observer, the median number of fixations ranged from 3 to 22 (Figs. 5A–5C).

To decide on a single criterion, we chose the combination of parameters that gave the highest partial AUC (pAUC calculated as AUC computed for specificities higher than 80%) and the highest specificity possible in our data was less than 100% (95.2%). It can be seen from Table 1 that the best criterion under this definition is with parameters $n = 2$ where $k \geq 3$ locations at $p = 99\%$ giving a sensitivity of 85% (95% CI, 70%–100%) with pAUC of 0.88 (95% CI, 0.75–0.98). The median number of the fixations for $n = 2$ and the measured proportion of correct across the 25 tested locations for all glaucoma participants are provided in Supplementary Tables S2 and S3. The results of the visual search task for the glaucoma cohort according to the final screening classification recommendation along with comparison to clinical visual field measure as measured with the HFA 10-2 SITA Standard protocol are shown in Figure 6.

Discussion

The current study aimed to develop a visual search task on a background with spatial frequency content representing natural scenes, with the number

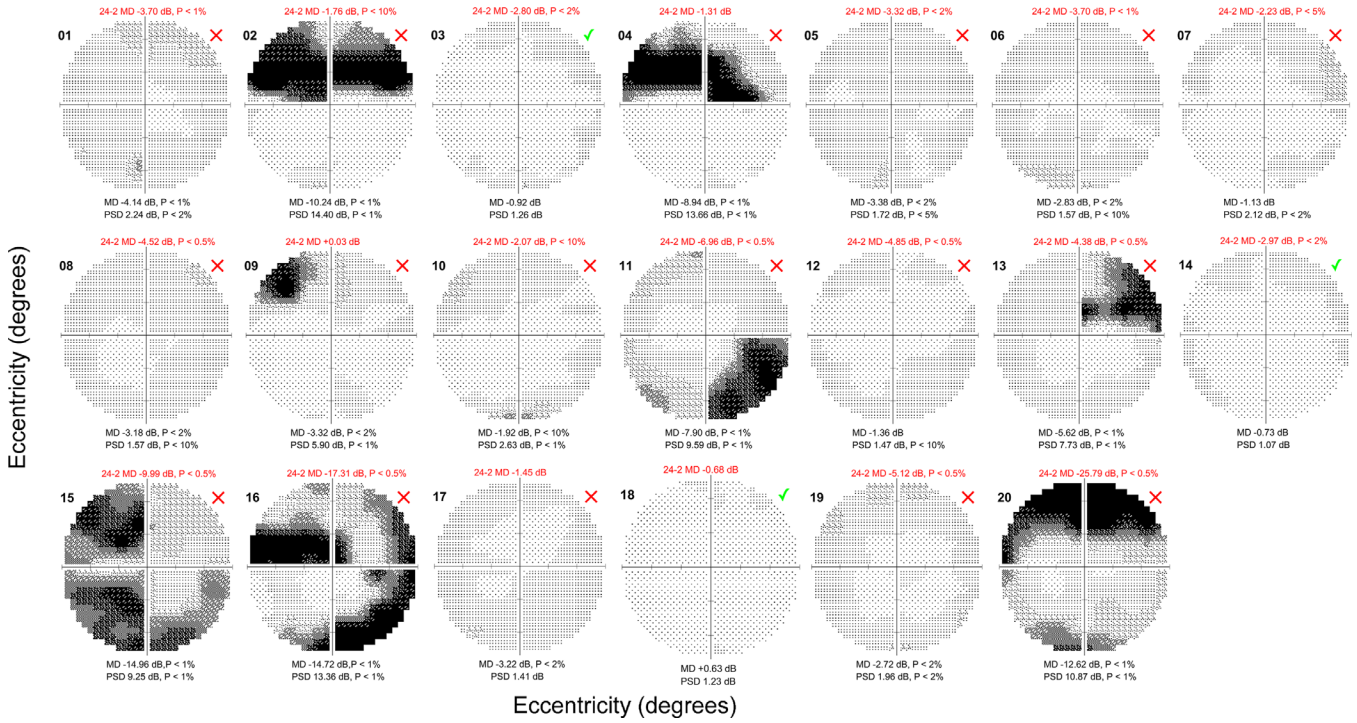

Figure 6. The results of the visual search task for each eye tested in the glaucoma cohort along with their visual field status as determined by standard automated perimetry. The grayscale picture represents the visual field status obtained from the HFA 10-2 SITA Standard with the corresponding 10-2 MD and PSD values in *black text*. The HFA 24-2 SITA Standard MD values of the participant are also provided in *red text*. A *green tick* indicates that the participant passed the visual search test according to the final screening classification recommendation, and the *red cross* indicates that the participant failed the test according to the final screening classification recommendation. MD, mean deviation; PSD, pattern standard deviation; dB, decibels. Grayscales were generated using software from Jones.[38]

of fixations made by the participants to find targets on the 1/f noise background as the outcome measure. We also evaluated whether the developed visual search task can be used to detect areas of abnormal central vision. Our results show that the current protocol can detect abnormal central visual field with 95.2% specificity and 85% sensitivity within an average time of about 1.5 minutes using low-cost hardware. The total testing time (median) taken by the control participants to perform the task for two trials was 85.71 (66.49–113.53) seconds.

It has been proposed that gaze scan paths/eye positions may be abnormal in people with visual field loss,[17] with previous studies demonstrating an increase in the number of fixations in people with visual field defects compared to controls when viewing a driving scene[22] or while performing a static visual search task.[39] In this study, we also demonstrated a higher number of fixations in glaucoma participants who had visual field defects (Fig. 6, Supplementary Tables S2, and S3).

Figure 6 shows that some of the glaucoma participants with normal 10-2 visual fields failed our screening assessment. There are several possible reasons for these glaucoma participants to fail the screening. First, four of the participants had macular defects noted on OCT (Fig. 6: 07, 08, 17, 19), specifically macular pucker. Three of these individuals had a 10-2 MD flagged at the $P < 2\%$ level, suggesting some generalized loss. It is also possible that the specific stimulus conditions of detecting stimuli on a nonuniform background results in reduced detectability of the target.[36] It is well known that presenting targets on complex backgrounds results in surround interactions.[31,40–42] Center surround interactions are known to vary with age,[43–47] and recently it has been shown that there are age and eccentricity interactions for detecting objects on stimulus conditions similar to the current study.[36] In this study, while the Gabor stimulus contrast and the on-average contrast of the 1/f background were fixed, the background noise images were selected at random from a battery of 1000 images generated randomly at the beginning of each experiment. Therefore local variations in the 1/f noise images may result in local differences in the relationship between the Gabor stimulus and its surround at a given location from trial to trial. We do not have sufficient replicates to explore whether there were any specific background images that resulted in unusual outcomes. Part of the rationale for the multisampling approach, and the random

selection of images on each presentation, is to ensure that the results are not peculiar to a specific noise background image.

In this study, we did not collect a true normative database. A representative normative database would require the collection of data on many individuals tested once. Instead, we pooled data from our 21 control participants each tested 20 times as a pragmatic substitute within this proof-of-concept study. Any future clinical application would require collection of age-relevant normative data and might result in slightly different cutoff limits than reported herein. Similarly, the selected single criterion for flagging a visual field test as abnormal (number of fixations greater than the $p = 99\%$ for $k = 3$ or more locations with $n = 2$ repeated presentations) may not prove to be the most appropriate criterion for future clinical application. Our intent is not to suggest final parameters for a clinical implementation of this procedure but to demonstrate that the approach shows promise for the detection of central visual field damage.

Here, we tested people with glaucoma to validate our screening approach. However, the visual search task was not designed to be a glaucoma-specific test. Indeed, the patients with macular pucker who failed our screening test suggest that the developed screening protocol may be widely useful for differentiating people with subtle visual functional abnormalities; however, more extensive trials are required to confirm. Because we were interested in the ability of the test to screen for visual disorder in general, we deliberately did not use the OCT macular scans for inclusion purposes in the glaucoma group. Instead, these were inspected to identify any ocular comorbidity that contributing to vision loss as the intent was to develop a screening tool that would direct people to have a full eye examination.

It is well known that contrast processing beyond standard perimetric targets is known to be impaired in glaucoma.[48–52] Consequently, there may be effects of glaucoma that are detected when a stimulus is presented on a nonuniform background, relative to standard perimetric testing. Further work is required to explore this possibility. The stimulus and behavioral methods used in this study were chosen based on prior work[30] that demonstrated a link between the detectability of targets within an image to the predicted number of fixations required to detect the target using visual search. We evaluated whether similar stimuli and methods could be used to identify central visual loss and therefore matched the field size to that prior work (15° in diameter). We anticipate that the methods can be used to assess a wider visual field angle, but additional data need to be collected to confirm this assertion. It is also worth noting that the target used in this study was six cycles/degree, which is a relatively high spatial frequency stimulus and therefore likely to be susceptible to cataract and metamorphopsia.[53,54] This was a deliberate and potentially useful feature, because the aim was to develop a screening test for visual disorder, rather than a specific test pertaining to glaucoma.

Given that the current screening test uses suprathreshold stimuli and does not have critical timing requirements in terms of stimulus display, the stimuli are suitable for standard monitors or tablets, connected to portable eye tracking devices. Using an eye tracker clipped onto a tablet has been demonstrated to be feasible for eye movement perimetry and has the potential to be used in settings such as triage in clinical waiting areas or for community vision screening.[12] Another alternative would be to incorporate the current screening protocol into existing virtual reality-based headset perimetry tests with eye-tracking capabilities.

In summary, in this study we created and tested a rapid screening test that uses visual search behavior to detect areas of abnormal central vision. The visual search task was designed to take advantages of the various features of natural vision, and to be easy and intuitive for participants. An advantage of the developed protocol is that performance might have more validity in relating to the quality-of-life measures or self-reported visual dysfunction than standard perimetry; however, this requires future research to establish.

Acknowledgments

Disclosure: **R. Srinivasan,** None; **A. Turpin,** None; **A.M. McKendrick,** None

References

1. Aspinall PA, Johnson ZK, Azuara-Blanco A, et al. Evaluation of quality of life and priorities of patients with glaucoma. *Invest Ophthalmol Vis Sci.* 2008;49:1907–1915.
2. Spaeth G, Walt J, Keener J. Evaluation of quality of life for patients with glaucoma. *Am J Ophthalmol.* 2006;141(1 Suppl):S3–S14.
3. Nelson P, Aspinall P, Papasouliotis O, et al. Quality of life in glaucoma and its relationship with visual function. *J Glaucoma.* 2003;12:139–150.
4. Wang Y, Alnwisi S, Ke M. The impact of mild, moderate, and severe visual field loss in glaucoma on patients' quality of life measured

via the Glaucoma Quality of Life-15 Questionnaire: a meta-analysis. *Medicine (Baltimore)*. 2017;96(48):e8019.
5. Artes PH, Iwase A, Ohno Y, et al. Properties of perimetric threshold estimates from full threshold, sita standard, and sita fast strategies. *Invest Ophthalmol Vis Sci.* 2002;43:2654–2659.
6. Johnson CA. Psychophysical factors that have been applied to clinical perimetry. *Vision Res.* 2013;90:25–31.
7. Troxler D. Ueber Das Verschwinden Gegebener Gegenstande Innerhalb Unseres Gesichtskreises. *Ophthalmologische bibliothek.* 1804;2:1–119.
8. Glen FC, Baker H, Crabb DP. A qualitative investigation into patients' views on visual field testing for glaucoma monitoring. *BMJ Open.* 2014;4(1):e003996.
9. Wood JM, Owens DA. Standard measures of visual acuity do not predict drivers' recognition performance under day or night conditions. *Optom Vis Sci.* 2005;82:698–705.
10. Owsley C, Ball K, Keeton DM. Relationship between visual sensitivity and target localization in older adults. *Vision Res.* 1995;35:579–587.
11. Wakayama A, Matsumoto C, Ohmure K, et al. Influence of background complexity on visual sensitivity and binocular summation using patterns with and without noise. *Invest Ophthalmol Vis Sci.* 2012;53:387–393.
12. Jones PR, Smith ND, Bi W, Crabb DP. Portable perimetry using eye-tracking on a tablet computer—a feasibility assessment. *Transl Vis Sci Technol.* 2019;8(1):17.
13. Jones PR, Lindfield D, Crabb DP. Using an open-source tablet perimeter (Eyecatcher) as a rapid triage measure for glaucoma clinic waiting areas. *Br J Ophthalmol.* 2021;105:681–686.
14. Asfaw DS, Jones PR, Edwards LA, et al. Using eye movements to detect visual field loss: a pragmatic assessment using simulated scotoma. *Sci Rep.* 2020;10(1):9782.
15. Gestefeld B, Grillini A, Marsman JC, Cornelissen FW. Using natural viewing behavior to screen for and reconstruct visual field defects. *J Vis.* 2020;20(9):11.
16. Meethal NSK, Pel JJM, Mazumdar D, et al. Eye movement perimetry and frequency doubling perimetry: clinical performance and patient preference during glaucoma screening. *Graefes Arch Clin Exp Ophthalmol.* 2019;257:1277–1287.
17. Crabb DP, Smith ND, Zhu H. What's on Tv? Detecting age-related neurodegenerative eye disease using eye movement scanpaths. *Front Aging Neurosci.* 2014;6:312.
18. Burton R, Crabb DP, Smith ND, et al. Glaucoma and reading: exploring the effects of contrast lowering of text. *Optom Vis Sci.* 2012;89:1282–1287.
19. Burton R, Smith ND, Crabb DP. Eye movements and reading in glaucoma: observations on patients with advanced visual field loss. *Graefes Arch Clin Exp Ophthalmol.* 2014;252:1621–1630.
20. Burton R, Saunders LJ, Crabb DP. Areas of the visual field important during reading in patients with glaucoma. *Jpn J Ophthalmol.* 2015;59:94–102.
21. Smith ND, Glen FC, Monter VM, Crabb DP. Using eye tracking to assess reading performance in patients with glaucoma: a within-person study. *J Ophthalmol.* 2014;2014:120528.
22. Crabb DP, Smith ND, Rauscher FG, et al. Exploring eye movements in patients with glaucoma when viewing a driving scene. *PLoS One.* 2010;5(3):e9710.
23. Lee SS, Black AA, Lacherez P, Wood JM. Eye movements and road hazard detection: effects of blur and distractors. *Optom Vis Sci.* 2016;93:1137–1146.
24. Lee SS, Black AA, Wood JM. Scanning behavior and daytime driving performance of older adults with glaucoma. *J Glaucoma.* 2018;27:558–565.
25. Wood JM, Black AA, Mallon K, et al. Effects of age-related macular degeneration on driving performance. *Invest Ophthalmol Vis Sci.* 2018;59:273–279.
26. Glen FC, Crabb DP, Smith ND, et al. Do patients with glaucoma have difficulty recognizing faces? *Invest Ophthalmol Vis Sci.* 2012;53:3629–3637.
27. Smith ND, Glen FC, Crabb DP. Eye movements during visual search in patients with glaucoma. *BMC Ophthalmol.* 2012;12(1):45.
28. Smith ND, Crabb DP, Garway-Heath DF. An exploratory study of visual search performance in glaucoma. *Ophthalmic Physiol Opt.* 2011;31:225–232.
29. Smith ND, Crabb DP, Glen FC, et al. Eye movements in patients with glaucoma when viewing images of everyday scenes. *Seeing Perceiving.* 2012;25:471–492.
30. Najemnik J, Geisler WS. Optimal eye movement strategies in visual search. *Nature.* 2005;434(7031):387–391.
31. Field DJ. Relations between the statistics of natural images and the response properties of cortical cells. *J Opt Soc Am A.* 1987;4:2379–2394.
32. Peirce JW. Psychopy—psychophysics software in Python. *J Neurosci Methods.* 2007;162(1-2):8–13.
33. Georgeson MA, Sullivan GD. Contrast constancy: deblurring in human vision by spatial frequency channels. *J Physiol.* 1975;252:627–656.

34. Webster MA, Miyahara E. Contrast adaptation and the spatial structure of natural images. *J Opt Soc Am A Opt Image Sci Vis.* 1997;14:2355–2366.
35. Jacob RJ. Eye tracking in advanced interface design. Barfield W, Furness TA, eds. In: *Virtual Environments and Advanced Interface Design*. New York: Oxford University Press, Inc., 1995:258–288.
36. Srinivasan R, Turpin A, McKendrick AM. Contrast sensitivity on 1/F noise is more greatly impacted by older age for the fovea than parafovea. *Optom Vis Sci.* 2021;98:394–403.
37. R Core Team. *R: A Language and Environment for Statistical Computing*. Vienna, Austria: R Foundation for Statistical Computing. Available at: https://wwwR-projectorg/. Accessed December 16, 2021.
38. Jones PR. Matlab Code for Generating Visual Field Greyscales from (Hfa) Perimetric Data. GitHub repository. Available at: https://github.com/petejonze/VfPlot. Accessed September 5, 2021.
39. Coeckelbergh TR, Cornelissen FW, Brouwer WH, Kooijman AC. The effect of visual field defects on eye movements and practical fitness to drive. *Vision Res.* 2002;42:669–677.
40. Lesica NA, Jin J, Weng C, et al. Adaptation to stimulus contrast and correlations during natural visual stimulation. *Neuron.* 2007;55:479–491.
41. Chubb C, Sperling G, Solomon JA. Texture Interactions Determine Perceived Contrast. *Proc Natl Acad Sci U S A.* 1989;86:9631–9635.
42. Angelucci A, Bijanzadeh M, Nurminen L, et al. Circuits and mechanisms for surround modulation in visual cortex. *Annu Rev Neurosci.* 2017;40:425–451.
43. Nguyen BN, McKendrick AM. Foveal and parafoveal contrast suppression are different: mechanisms revealed by the study of healthy aging. *J Vis.* 2016;16(3):10.
44. Malavita MS, Vidyasagar TR, McKendrick AM. The effect of aging and attention on visual crowding and surround suppression of perceived contrast threshold. *Invest Ophthalmol Vis Sci.* 2017;58:860–867.
45. Yazdani P, Serrano-Pedraza I, Whittaker RG, et al. Two common psychophysical measures of surround suppression reflect independent neuronal mechanisms. *J Vis.* 2015;15(13):21.
46. Karas R, McKendrick AM. Aging alters surround modulation of perceived contrast. *J Vis.* 2009;9(5):11.
47. Karas R, McKendrick AM. Increased surround modulation of perceived contrast in the elderly. *Optom Vis Sci.* 2011;88:1298–1308.
48. McKendrick AM, Sampson GP, Walland MJ, Badcock DR. Contrast sensitivity changes due to glaucoma and normal aging: low-spatial-frequency losses in both magnocellular and parvocellular pathways. *Invest Ophthalmol Vis Sci.* 2007;48:2115–2122.
49. Sampson GP, Badcock DR, Walland MJ, McKendrick AM. Foveal contrast processing of increment and decrement targets is equivalently reduced in glaucoma. *Br J Ophthalmol.* 2008;92:1287–1292.
50. Lek JJ, Vingrys AJ, McKendrick AM. Rapid contrast adaptation in glaucoma and in aging. *Invest Ophthalmol Vis Sci.* 2014;55:3171–3178.
51. McKendrick AM, Sampson GP, Walland MJ, Badcock DR. Impairments of contrast discrimination and contrast adaptation in glaucoma. *Invest Ophthalmol Vis Sci.* 2010;51:920–927.
52. McKendrick AM, Badcock DR, Morgan WH. Psychophysical measurement of neural adaptation abnormalities in magnocellular and parvocellular pathways in glaucoma. *Invest Ophthalmol Vis Sci.* 2004;45:1846–1853.
53. Owsley C, Sekuler R, Siemsen D. Contrast sensitivity throughout adulthood. *Vision Res.* 1983;23:689–699.
54. Elliott DB. Evaluating visual function in cataract. *Optom Vis Sci.* 1993;70:896–902.